Investigating Printability of Native Defects on EUV Mask Blanks through Simulations and Experiments

Mihir Upadhyaya[1], Vibhu Jindal[2], Henry Herbol[1], Il-Yong Jang[2], Hyuk Joo Kwon[2], Jenah Harris-Jones[2], Gregory Denbeaux[1]

[1]College of Nanoscale Science and Engineering, University at Albany,
255 Fuller Road, Albany, New York, 12203, USA
[2]SEMATECH
257 Fuller Rd, Albany, NY 12203, USA

ABSTRACT

Availability of defect-free masks is considered to be a critical issue for enabling extreme ultraviolet lithography (EUVL) as the next generation technology. Since completely defect-free masks will be hard to achieve, it is essential to have a good understanding of the defect printability as well as the fundamental aspects of a defect that result in the defects being printed. In this work, the native mask blank defects were characterized using atomic force microscopy (AFM) and cross-section transmission electron microscopy (TEM), and the defect printability of the characterized native mask defects was evaluated using finite-difference time-domain (FDTD) simulations. The simulation results were compared with the through-focus aerial images obtained at the SEMATECH Actinic Inspection Tool (AIT) at Lawrence Berkeley National Lab (LBNL) for the characterized defects. There was a reasonable agreement between the through-focus FDTD simulation results and the AIT results. To model the Mo/Si multilayer growth over the native defects, which served as the input for the FDTD simulations, a level-set technique was used to predict the evolution of the multilayer disruption over the defect. Unlike other models that assume a constant flux of atoms (of materials to be deposited) coming from a single direction, this model took into account the direction and incident fluxes of the materials to be deposited, as well as the rotation of the mask substrate, to accurately simulate the actual deposition conditions. The modeled multilayer growth was compared with the cross-section TEM images, and a good agreement was observed between them.

INTRODUCTION

Extreme ultraviolet lithography (EUVL) is the leading next generation lithography technology to succeed optical lithography beyond the 16 nm technology node [1, 2, 3]. The reflective masks used in EUVL consist of a low thermal expansion glass substrate coated with a Mo/Si multilayer and a patterned absorber layer. The availability of defect-free mask blanks is one of the most critical technology gaps hindering the commercialization of EUVL [2, 3]. The defects namely the pit or particle, can originate either on the substrate, during multilayer deposition, or on top of the multilayer stack [4, 5, 6].

The physical structure of a defect produced by a particle within the multilayer coating of an EUVL mask can be complex. In order to determine the smallest particle capable of producing a printable defect, it is crucial to be able to model the growth as well as the printability of the defects accurately. Modeling is also essential in determining strategies to mitigate the printability

Extreme Ultraviolet (EUV) Lithography V, edited by Obert R. Wood II, Eric M. Panning, Proc. of SPIE
Vol. 9048, 90483L · © 2014 SPIE · CCC code: 0277-786X/14/$18 · doi: 10.1117/12.2057761

Downloaded From: http://spiedigitallibrary.org/ on 11/21/2015 Terms of Use: http://spiedigitallibrary.org/ss/TermsOfUse.aspx

of such defects by employing various techniques like defect smoothing [7], multilayer defect compensation technique [8], or using additional buffer layer [9], to name a few.

The most commonly used model, namely the non-linear continuum model or the Stearns model [10] used to simulate the multilayer growth over a defect, does not take into account the tool deposition conditions. In the model used [11] here, we took into account the tool deposition conditions which include the angular flux of atoms incident on the substrate, the chamber geometry and various other deposition factors such as substrate and target angle, substrate and target size, and the distances.

The model developed here (also true for the Stearns model) overcomes the limitations of techniques like the single surface approximation (SSA) and the conformal multilayer growth techniques which attempt to approximate the defect propagation through the multilayer stack. In SSA, the defective multilayer structure is replaced by a single reflecting surface with the shape of the top surface of the multilayer. This approximation is valid only for low aspect ratio defects [12]. The conformal multilayer growth assumes the defect to be uniformly propagated through the multilayer stack. Again, this approximation only holds true for small defects [10].

The aim of our work was to draw comparisons between the aerial images obtained using AIT tool at LBNL and those obtained using the FDTD simulations that used the level-set modeled multilayer growth as the input. We obtained a reasonable match between the two.

CHARACTERIZATION OF NATIVE DEFECTS ON EUV MASK BLANK

Once the multilayer deposition process on the mask substrate was complete, the mask blank was analyzed for defects using a Lasertec M7360 inspection tool which uses light scattering as a means to detect defects present on the substrate surface. The defect location was marked with the help of fiducials to easily locate the defect for AFM, TEM and AIT printability studies. Once the multilayers and the capping layer were deposited, AFM was performed at the defect location to observe the defect profile on top of the mask blank. The masks were then sent to LBNL for defect printability studies on the AIT inspection tool where the aerial images of the defect sites were obtained at multiple focus conditions. TEM cross section studies were then performed on the defects to observe how the multilayer deforms as the defect propagates up the multilayer stack. The defect profile at the substrate obtained from the TEM was used as one of the inputs into the multilayer growth model.

MULTILAYER GROWTH MODEL

The multilayer growth model, as developed [11], looked at the deposition conditions of the Veeco Instruments' Nexus low defect density (LDD) tool located in the SEMATECH cleanroom facility. The tool basically consists of an ion source, Si, Mo and Ru targets, and an electrostatic chuck to hold the mask substrate. The schematic of the tool is shown in Figure 1. Ar ions strike the target liberating the atoms to be deposited. The atoms travel to the mask substrate where they adsorb, creating the multilayer reflector. The mask substrate is electrostatically chucked to the

Downloaded From: http://spiedigitallibrary.org/ on 11/21/2015 Terms of Use: http://spiedigitallibrary.org/ss/TermsOfUse.aspx

mask fixture, which precisely positions the substrate relative to the target and spins the substrate around its normal direction.

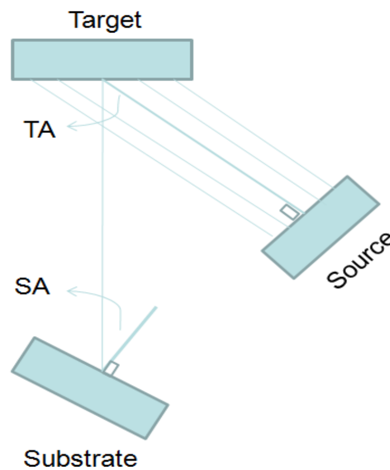

Figure 1: Schematic of the Ion Beam Deposition tool.

The multilayer growth model uses kinetic Monte Carlo methods, taking into account the sputtered flux, energy of the sputtered atoms, and gas scattering inside the chamber. The model tracks atoms as they are ejected from the target and pass through the vacuum inside the chamber. It takes into account the probability of striking an ambient gas atom along the atom's trajectory and predicts the energy and direction of the atom after the collision. The atom is tracked until it strikes a surface where it is assumed to stick, and its position is recorded. The scattering gas in the initial simulations was assumed to have a Boltzmann's velocity distribution at 50°C and to be comprised of argon atoms at 0.14 mTorr, which is the pressure inside the Veeco chamber during deposition. Modeling the deposition rate throughout the chamber requires estimates of several parameters, such as the number of atoms ejected from the target at each location on the target which was estimated using measured target erosion profiles; the angular distribution of atoms reaching the substrate which was estimated by measuring the deposition rate on substrates mounted on a hemispherical surface around the center of the target; the gas scattering behavior between the target and substrate which was estimated using a kinetic Monte Carlo method and scattering cross sections. The sputtered or scattered atoms that hit any surface (chamber components or substrate surface) are assumed to stick. A collision kinetic theory with a random impact parameter was used to determine the post-collision velocity of the atom. The deposition model records the position of the atoms that strike the substrate. The substrate rotation that is commonly used to improve uniformity in the Veeco Nexus tools is modeled by rotationally averaging the number of atoms that strike the substrate. Typically 40,000,000 atoms are launched to get reasonable statistics on substrate uniformity.

After determining the growth rates and uniformity on the multilayer, one can simulate multilayer growth on a given defect profile. Level set method is used to simulate defect growth during multilayer deposition. Simulations of defect shape and growth during this deposition take into account the nature and profile of the defect (pit or bump) and direction and incident flux of the material, based on the deposition conditions.

Downloaded From: http://spiedigitallibrary.org/ on 11/21/2015 Terms of Use: http://spiedigitallibrary.org/ss/TermsOfUse.aspx

RESULTS

a. Comparing the Modeled Multilayer Growth with the Cross Section TEM Images:

The level-set deposition model was able to predict the deposition rate and uniformity of the material deposited on the mask substrate. TEM cross section through the defect was performed and the defect profile at the substrate obtained from the TEM served as the input into our multilayer growth simulation. The TEM cross section of the defect appears to agree with the simulated multilayer growth over the defect as shown in Figure 2. However, with more accurate AFM measurements of the top surface of the defect, we find a mismatch of around 20% in the height and FWHM of the defect at the surface. Multilayer growth of 40 Mo/Si multilayers was modeled with each bilayer being approximately 7 nm thick. Although the parameters used here were those of the Veeco Nexus tool, the model can simulate multilayer growth under different deposition conditions in different tools.

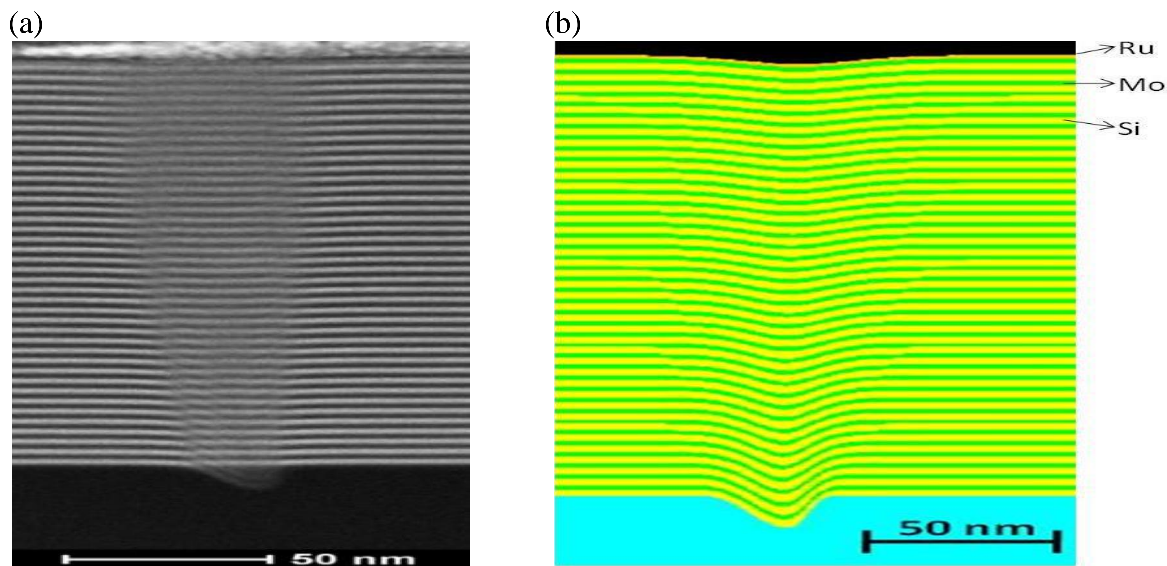

Figure 2: (a) TEM cross-section of the pit-type defect on the EUV mask. (b) Simulated multilayer growth over the pit-type defect using our model.

b. Comparing the FDTD Simulation and AIT Through-focus Aerial Images:

The simulated multilayer growth was used as the input for the FDTD simulations. To perform the FDTD simulations, EM-SUITE, a lithographic software developed by Panoramic Technology Inc. was used. The optical and imaging parameters used for the simulations were chosen to match the parameters used for the AIT imaging, which were 13.4 nm wavelength radiation incident on the mask at an angle of 6 degrees, top-hat illumination with a sigma value of 0.15, numerical aperture of 0.35, and a demagnification factor of 4. Figure 3 shows the aerial images from the AIT along with the aerial images obtained from the FDTD simulations. We observe a reasonable match between the through-focus aerial image intensities obtained at AIT and obtained using the FDTD simulations. We however do not have an ideal match between the FDTD and the AIT results, as is evident from Figure 3(b). This, we believe, is primarily due to the fact that the defect profile used as the input for the multilayer growth model was not an ideal representation of the defect structure at the substrate. The TEM cross section obtained might not

Downloaded From: http://spiedigitallibrary.org/ on 11/21/2015 Terms of Use: http://spiedigitallibrary.org/ss/TermsOfUse.aspx

have been through the center of the defect thus leading to an inaccurate assessment of the substrate defect profile. This would lead to an inaccuracy in determining the defect profile at the top of the multilayer stack. This was confirmed by the fact that the FWHM of the defect at the top of the multilayer stack as determined by AFM measurements had a value of 44.1nm as opposed to the FWHM value of 36nm obtained from the modeled multilayer growth. Also, the defect depth at the top of the multilayer stack as determined by the AFM was 7.4nm as opposed to a depth of 5.7nm as predicted by the multilayer growth model. This, we believe is the most plausible reason for the non-ideal match between the simulation and the AIT data, and the determination of the defect profile at the substrate needs to be more accurate in order to obtain a better match, ideally with an AFM measurement of the defect at the mask substrate.

(a)

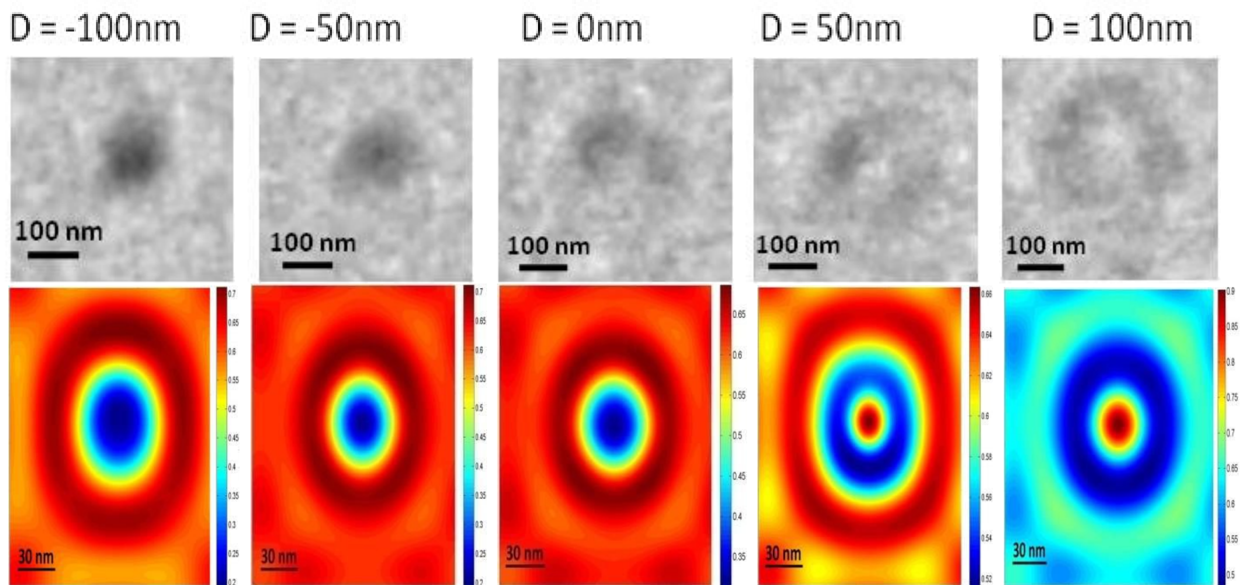

(b)

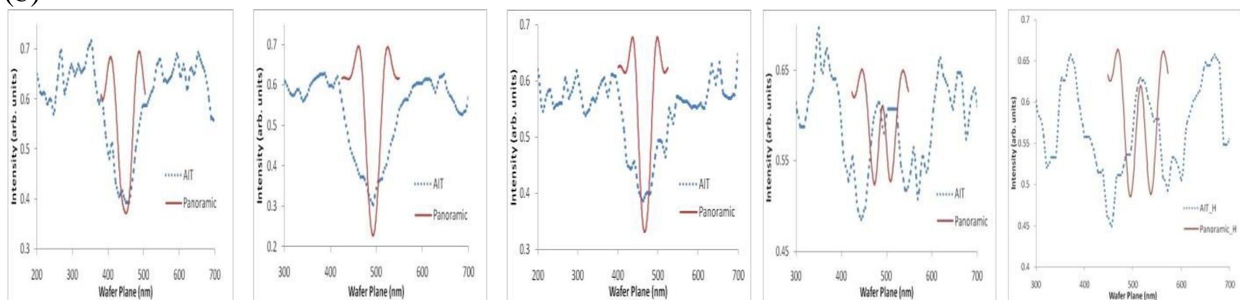

Figure 3: (a) 2-D aerial image intensity data obtained at AIT and using FDTD simulations (below). (b) 1-D aerial image intensity data extracted from the 2-D aerial image intensity maps obtained at AIT and through FDTD simulations. 'D' in the figure refers to the defocus values in nanometers. We observe the intensity drop from the FDTD simulations and AIT imaging to be similar in height, however not in width.

Downloaded From: http://spiedigitallibrary.org/ on 11/21/2015 Terms of Use: http://spiedigitallibrary.org/ss/TermsOfUse.aspx

CONCLUSION

We obtained a reasonable match between the through-focus aerial image data obtained at AIT and the FDTD simulation results for the characterized native mask defect, using the multilayer growth model that took into account the deposition conditions of the ion beam deposition tool where the multilayer deposition took place. However, we did not obtain an ideal match between the AIT and the simulation data, we believe, due to an imperfect substrate defect profile that served as the input into the level-set growth model, which in turn served as the input into our FDTD simulations. The data presented here is preliminary, and our goal going forward is to perform better metrology to obtain the accurate defect profile at the substrate, so that we can obtain a better match between the FDTD and the AIT data.

REFERENCES

[1] B. LaFontaine, Y. Deng, R.-H. Kim, H. J. Levinson, S. McGowan, U. Okoroanyanwu, R. Seltmann, C. Tabery, A. Tchikoulaeva, T. Wallow, O. Wood, J. Arnold, D. Canaperi, M. Colburn, K. Kimmel, C.-S. Koay, E. McLellan, D. Medeiros, S. P. Rao, K. Petrillo, Y. Yin, H. Mizuno, S. Bouten, M. Crouse, A. van Dijk, Y. van Dommelen, J. Galloway, S.-I. Han, B. Kessels, B. Lee, S. Lok, B. Niekrewicz, B. Pierson, R. Routh, E. Schmit-Weaver, K. Cummings and J. Word, *The use of euv lithography to produce demonstration devices*, Proc. SPIE, **6921**, 69210P (2008).

[2] O. Wood, C.-S. Koay, K. Petrillo, H. Mizuno, S. Raghunathan, J. Arnold, D. Horak, M. Burkhardt, G. McIntyre, Y. Deng, B. La Fontaine, U. Okoroanyanwu, T. Wallow, G. Landie, T. Standaert, S. Burns, C. Waskiewicz, H. Kawasaki, J. H. C. Chen, M. Colburn, B. Haran, S. S. C. Fan, Y. Yin, C. Holfeld, J. Techel, J.-H. Peters, S. Bouten, B. Lee, B. Pierson, B. Kessels, R. Routh and K. Cummings, *Euv lithography at the 22nm technology node*, Proc. SPIE, **7636**, 76361M (2010).

[3] S. Wurm, C.-U. Jeon and M. Lercel, *Sematech's euv program: A key enabler for EUVL introduction*, Proc. SPIE, **6517**, 651705 (2007).

[4] P. B. Mirkarimi and D. G. Stearns, *Investigating the growth of localized defects in thin films using gold nanospheres*, Appl. Phys. Lett., **77**, 2243 (2000).

[5] R. V. Randive, A. Ma, P. A. Kearney, D. Krick, I. Reiss, P. B. Mirkarimi and E. Spiller, *Progress in the fabrication of low-defect density mask blanks for extreme ultraviolet lithography*, J. Microlith. Microfab. Microsyst., **5**, 023003 (2006).

[6] Y. Lin and J. Bokor, *Minimum critical defects in extreme-ultraviolet lithography masks*, J. Vac. Sci. Technol. B, **15**, 2467 (1997).

[7] J. H-Jones, V. Jindal, P. Kearney, R. Teki, A. John and H.J. Kwon, *Smoothing of substrate pits using ion beam deposition for EUV lithography*, Proc. SPIE, **8322**, 83221S (2012).

Downloaded From: http://spiedigitallibrary.org/ on 11/21/2015 Terms of Use: http://spiedigitallibrary.org/ss/TermsOfUse.aspx

[8] T. Liang and E. Gullickson, *Multilayer defect compensation to enable quality masks for EUV production*, International Symposium for EUV Lithography, Lake Tahoe, California, 2008.

[9] B.T. Lee, E. Hoshino, M. Takahashi, T. Yoneda, H. Yamanashi, H. Hoko, A. Chiba, M. ito, M. Ryoo, T. Ogawa and S. Okazaki, *Characteristics of the Ru buffer layer for EUVL mask patterning*, Proc. SPIE, **4343**, 746 (2001).

[10] D.G. Stearns, P.B. Mirkarimi and E. Spiller, *Localized defects in multilayer coatings*, Thin Solid Films, **446**, 37 (2004).

[11] V. Jindal, P. Kearney, J. Harris-Jones, A. Hayes and J. Kools, *Modeling the EUV Multilayer Deposition Process on EUV Blanks*, Proc. SPIE **7969**, 79691A (2011).

[12] E.M Gullikson, C. Cerjan, D.G. Stearns, P.B. Mirkarimi and D.W. Sweeney, *Practical approach for modeling EUVL mask defects*, J. Vac. Sci. Technol. B, **20**, 81 (2002).

Downloaded From: http://spiedigitallibrary.org/ on 11/21/2015 Terms of Use: http://spiedigitallibrary.org/ss/TermsOfUse.aspx